Geophysical Research Letters

RESEARCH LETTER
10.1029/2025GL117821

Runaway Cooling From Large Solar Reductions Modulated by Ocean Overturning Circulation and Heat Uptake

Maya V. Chung[1,2], **Wenchang Yang**[3], **and Gabriel A. Vecchi**[1,2,3]

[1]Program in Atmospheric and Oceanic Sciences, Princeton University, Princeton, NJ, USA, [2]High Meadows Environmental Institute, Princeton University, Princeton, NJ, USA, [3]Department of Geosciences, Princeton University, Princeton, NJ, USA

Key Points:

- Two climate models have different responses to extreme solar reductions driven by ice-albedo feedback
- Ice cover and surface temperature differences are influenced by ocean heat uptake and one model's transient Pacific overturning
- Pacific overturning formation associated with lower salinity stratification in the north Pacific

Supporting Information:

Supporting Information may be found in the online version of this article.

Correspondence to:

M. V. Chung,
mvchung@princeton.edu

Citation:

Chung, M. V., Yang, W., & Vecchi, G. A. (2025). Runaway cooling from large solar reductions modulated by ocean overturning circulation and heat uptake. *Geophysical Research Letters*, *52*, e2025GL117821. https://doi.org/10.1029/2025GL117821

Received 1 JUL 2025
Accepted 15 SEP 2025

Abstract The climate system can respond asymmetrically to warming and cooling, yet this asymmetry remains underexplored. This study uses multi-century experiments with two coupled global climate models under idealized abrupt solar forcing changes of ±1%, 2%, 4%, and 6%. In both models, cooling has a larger impact on surface temperature than warming, driven by the ice-albedo feedback. However, under strong cooling (−4%, −6% Solar), the models diverge significantly. One model undergoes runaway ice growth, while the other has slower ice expansion and even transient sea ice retreat in the north Pacific. The latter is linked to the development of a strong Pacific meridional overturning circulation, which transports heat northward and slows ice growth. The model with less ice growth also exhibits greater "cold uptake into" (or heat release from) the deep ocean. These findings motivate further investigation of inter-model differences in ocean-ice-atmosphere interactions and their impacts on climate feedbacks.

Plain Language Summary Understanding both warming and cooling of the climate system is crucial for studying past climates, predicting climate changes under different greenhouse gas emission scenarios, and connecting past climates to future changes. This study compares how two climate models respond to sudden increases and decreases in incoming sunlight. While both models show similar warming and moderate cooling responses, they behave differently under strong cooling. In one model, sea ice rapidly expands and reaches the tropics within a few centuries, whereas in the other, ice growth never reaches that point even after running the simulations for nearly twice as long. We find that in the second model, an ocean overturning circulation develops in the Pacific that transports heat from the Equator northward. This process prevents sea ice from advancing by melting it from below. These findings emphasize the need to examine the ocean's role in climate change, run models for multiple centuries, and conduct more simple perturbation experiments including cooling scenarios to better understand discrepancies between climate models.

1. Introduction

Cooling in the climate system has received less research focus than global warming. Yet, it is critical for understanding past climates and may grow more relevant if emissions decline or for assessing geoengineering to counter warming. Several early studies examined how decreasing solar radiation affects climate to better understand ice ages and investigate asymmetries between warming and cooling. These studies used various complexities of climate models, such as zonal mean energy balance models (e.g., Budyko, 1969; Held & Suarez, 1974; Sellers, 1969), 2-level dynamic and diffusive models (Held et al., 1981), coarse-resolution 3D atmospheric global climate models (GCMs) (Wetherald & Manabe, 1975), and GCMs with simplified interactive oceans (Sellers, 1983, 1985). The ice-albedo feedback was consistently found to amplify cooling more strongly than warming, and the response was sensitive to atmospheric diffusivity and meridional heat transport. However, many of these studies were limited by computational constraints and simplified ocean representations, which prevented a realistic characterization of the transient and equilibrium climate response.

More recent work has shown that ocean dynamics can shape the climate's long-term response to radiative forcing. Early multi-century coupled GCM experiments found that ocean vertical mixing was a major driver of surface temperature evolution under warming and cooling (Stouffer, 2004), and subsequent studies demonstrated the ocean's slow influence on climate feedbacks and spatial patterns of warming (Armour et al., 2013; Held et al., 2010; Proistosescu & Huybers, 2017; Rose et al., 2014; Winton et al., 2010). Still, many climate feedback analyses span relatively short timescales (≤150 years), limiting their ability to capture the full ocean response.

The ocean overturning, including the Atlantic meridional overturning circulation (AMOC), redistributes heat in the climate system in complex ways (e.g., Mitevski et al., 2021; Stouffer, 2004; Stouffer & Manabe, 2003). Under warming, the AMOC has been found to have different transient and equilibrium responses depending on regional temperature and salinity changes, which may require millennial simulations to resolve (e.g., Bonan et al., 2022; Curtis & Fedorov, 2024a; Haskins et al., 2019; Jansen et al., 2018).

Newer studies have used modern GCMs and advanced diagnostic methods to analyze climate feedbacks under both warming and cooling. Kay et al. (2024) explored the long-term response to abrupt CO_2 doubling and halving, finding that under cooling, the albedo and lapse-rate feedbacks contributed most to climate instability, with AMOC changes having a secondary impact. Eisenman and Armour (2024) explored a wider range of transient CO_2 scenarios and found the same feedbacks dominated under cooling, although they did not explicitly analyze AMOC.

This study builds on previous work by exploring several warming and cooling perturbations and assessing transient and equilibrating responses using long model integrations (200–1,900 years). In contrast to most previous studies, we directly compare two GCMs to evaluate the robustness of feedbacks across different model formulations. Our experiments involve abrupt changes in the solar constant by ±1%, 2%, 4%, and 6%, ensuring a more consistent change in top-of-atmosphere (TOA) radiative forcing across models, unlike CO_2 forcing, which varies across models. We find that under strong cooling, the two models differ greatly in stability due to differences in the ice-albedo feedback. In the more stable model, sea ice expansion is suppressed by a transient Pacific meridional overturning circulation (PMOC) that transports heat poleward, and the surface temperature response is moderated by enhanced heat release from the deep ocean ("cold uptake"). We analyze the drivers of these circulation differences and discuss their implications for climate stability.

2. Data and Methods

2.1. Global Climate Models

This study uses two GCMs from the Geophysical Fluid Dynamics Laboratory: CM2.1 (Delworth et al., 2006) and the CM2.5 Forecast-oriented Low Ocean Resolution (FLOR) model (Vecchi et al., 2014). Both models have a fully coupled atmosphere and ocean. FLOR has higher horizontal resolution in the atmosphere and land (50 km) compared to CM2.1 (2°), while the models have the same ocean resolution (1°, with 1/3° meridional resolution near the Equator and 10 m vertical resolution in the surface ocean). Though these models are part of a common development tree, CM2.1 and FLOR are different model versions and differ in key dynamical representations and parameterizations, including ocean mixing schemes.

2.2. Abrupt Solar Perturbation Experiments

All model runs begin from a Control experiment with 1,860 radiative forcing conditions and are spun up for 100 years, which are excluded from the analysis. The Control simulations are run for an additional 2,900 years in FLOR and 3,900 years in CM2.1. After an initial adjustment, both control experiments exhibit minimal global temperature drift (about 0.5°C per 1,000 years).

The perturbation experiments abruptly change the solar constant ($S_0 = 1366$ W m^{-2}) by ±1%, 2%, 4%, and 6%. For a perturbation of X%, the solar constant becomes:

$$S = S_0(1 + 0.01X) \quad (1)$$

This results in TOA insolation changes of about 3.5 W m^{-2} per percentage point (1,860 Control insolation is 341.5 W m^{-2}), impacting the mean solar forcing and the amplitude of the annual and diurnal cycles.

Each multi-century experiment was performed for a different length of time (Figure 1). Some simulations failed due to the extreme forcing (Text S1 in Supporting Information S1) while others were intentionally stopped due to data storage constraints. For the CM2.1 –6% Solar experiment, three additional ensemble members were initialized from Control years 1,001, 2,001, and 3,001 and run for ≥900 years to examine the robustness of the development of PMOC.

10.1029/2025GL117821

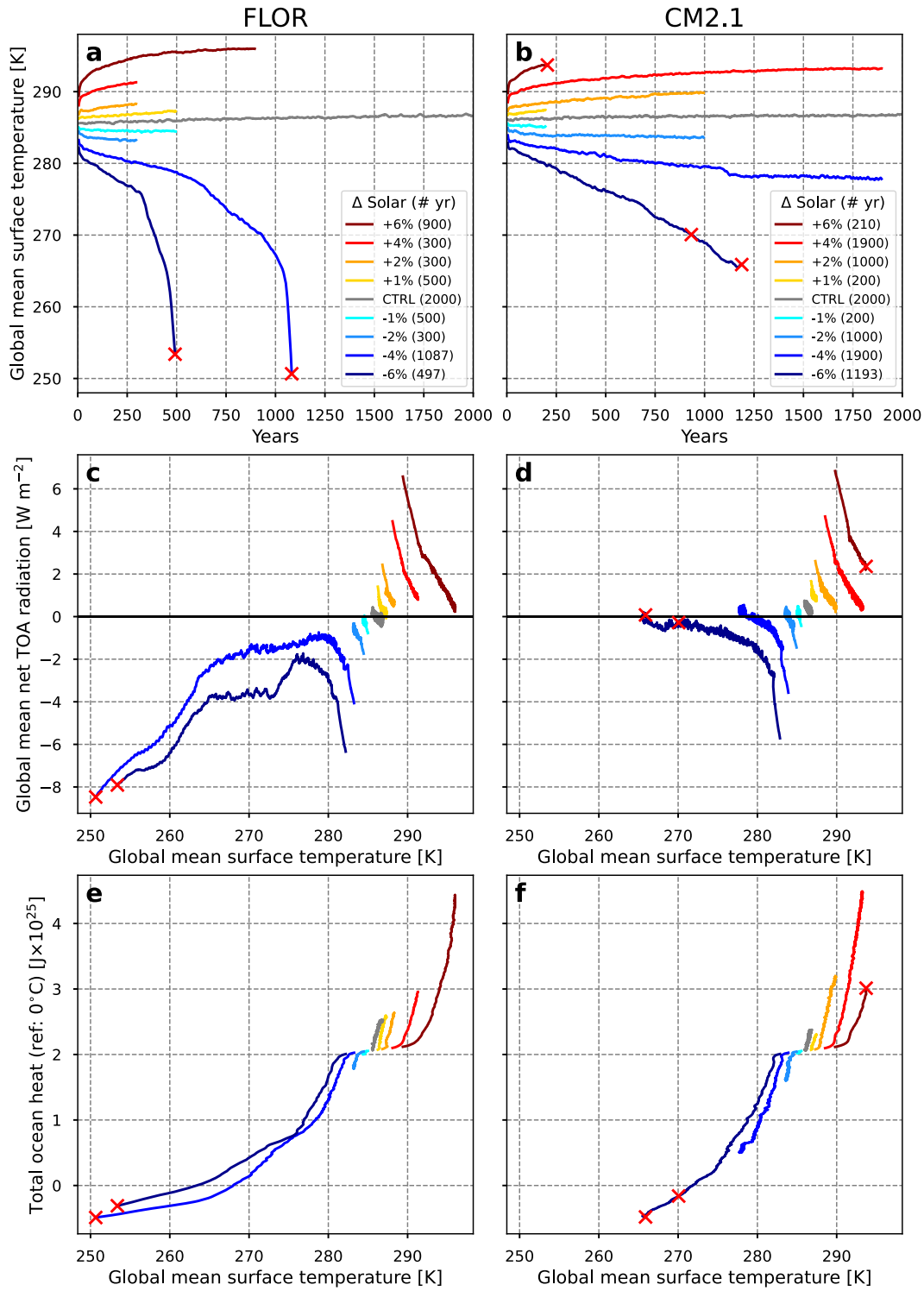

Figure 1. Solar experiments in the CM2.5 Forecast-oriented Low Ocean Resolution (FLOR) model (a,c,e) and CM2.1 (b, d, f). (a, b) Global mean surface temperature (GMST) over time. (c, d) Global mean net top-of-atmosphere radiation versus GMST. (e, f) Total ocean heat content referenced to 0°C versus GMST. All values are 10-year running means. Red × denotes experiment crashes (see Text S1 in Supporting Information S1).

2.3. Climate Feedbacks

The TOA radiation imbalance N may be written as:

$$N = F - \alpha \mathrm{d}T \tag{2}$$

where F is the effective forcing, $\mathrm{d}T$ is the surface air temperature change, α is the climate feedback parameter, and N, F, and $\mathrm{d}T$ are global means. α is computed as the slope of an ordinary least squares regression of the change in the annual global mean TOA radiative response ($\mathrm{d}R$) against $\mathrm{d}T$:

$$\alpha = \frac{\mathrm{d}R}{\mathrm{d}T} \tag{3}$$

where $\mathrm{d}R$ and $\mathrm{d}T$ are computed relative to a 50-year running mean Control climatology updated every 5 years, to account for model drift in the multi-century runs. This approach is most similar to the "differential feedback" described in Rugenstein and Armour (2021).

The total radiative response $\mathrm{d}R$ is computed as the sum of the radiative responses associated with changes in surface temperature (Planck), atmospheric lapse rate, relative humidity, surface albedo, and clouds, using the GFDL radiative kernel and direct computation of the cloud radiative response, following Soden et al. (2008). This analysis uses the relative humidity decomposition, which separates the impact of atmospheric warming on radiation from changes in relative humidity (relative humidity feedback), if one assumes relative humidity remains constant as surface and atmospheric temperature changes (lapse rate feedback) (Held & Shell, 2012). The conventional decomposition yields qualitatively similar results (e.g., Wang et al., 2025).

Note that the kernel method and feedback framework assume linearization around a climate near present day, which may limit their applicability to the more extreme experiments. Applying these frameworks is meant to be a starting point to understand the basic differences in feedbacks between the experiments.

2.4. Ocean Heat Uptake Efficiency

The ocean heat uptake efficiency (OHUE), κ (W m^{-2} K^{-1}), is computed as the ratio of the change in global ocean heat uptake (OHU) to the surface air temperature change:

$$\kappa = \frac{\mathrm{d}OHU}{\mathrm{d}T} \tag{4}$$

where the changes are calculated as an anomaly relative to the Control climatology as with α. α and κ represent how atmospheric radiative processes and oceanic processes affect $\mathrm{d}T$, with positive values indicating stabilization. Because this simplified framework does not consider vertical gradients in OHU, we additionally examine ratios between deep and upper OHU in Results Section 3.2.

3. Results

3.1. Global Energy Balance and Feedbacks

The Solar experiments reveal significant inter-model differences in surface temperature and TOA energy imbalance, particularly under strong cooling. Both models respond similarly to warming and moderate cooling (−1%, −2%) (Figures 1a and 1b). However, under extreme cooling (−4%, −6%), after a few centuries, FLOR exhibits runaway cooling and sea ice growth and increasing TOA imbalance (Figure 1c), whereas CM2.1 exhibits more stabilizing cooling, even when run about twice as long. Additional CM2.1%–6% Solar ensemble members confirm no runaway cooling within about 1,000 years (Figure S1 in Supporting Information S1).

In FLOR, the runaway cooling under −4% and −6% Solar is characterized by a large destabilizing (negative) total climate feedback (α, Figure 2a). In contrast, CM2.1 approaches near-equilibrium conditions; its net TOA imbalance trends toward zero (Figure 1d), and its total climate feedback tends to be more stable (positive) than FLOR (Figure 2b).

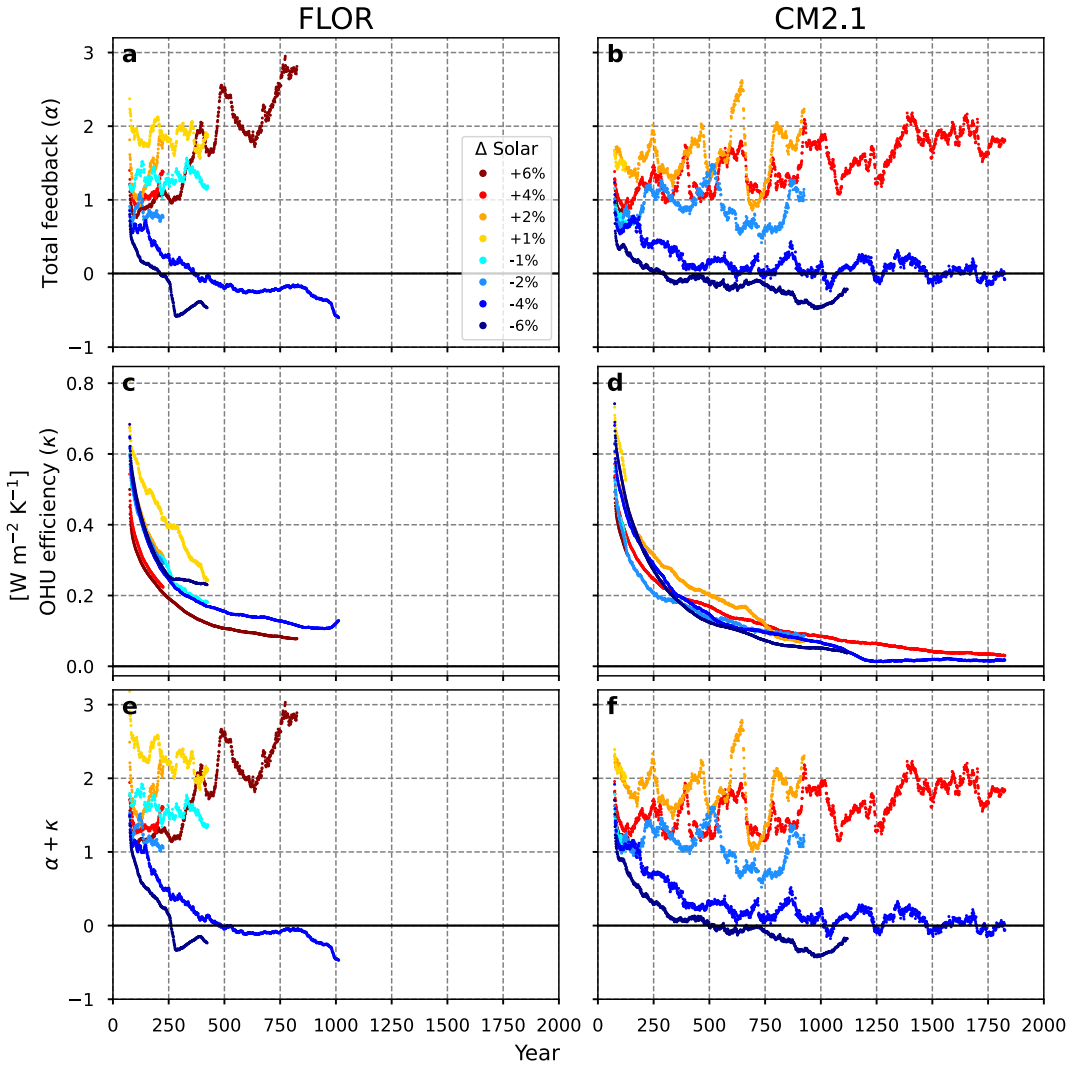

Figure 2. Feedbacks and ocean heat uptake efficiency (OHUE) in the CM2.5 Forecast-oriented Low Ocean Resolution (FLOR) model (a, c, e) and CM2.1 (b, d, f) Solar experiments. (a, b) Total climate feedback α. (c, d) OHUE κ. (e, f) Sum of α and κ. All values are relative to the Control 50-year mean climatology updated every 5 years. The feedbacks are computed using a 150-year moving window for the linear regression, and the OHUE is smoothed using a 150-year sliding window.

Inter-model differences in OHU appear to contribute to these divergent responses. CM2.1 "takes up more cold" into (releases more heat from) the ocean interior than FLOR (Figures 1e and 1f) per degree of surface temperature change. This is reflected in CM2.1's relatively high OHUE, at least for the first few hundred years of the experiments (κ, Figures 2c and 2d). $\kappa + \alpha$ is the "climate resistance" (e.g., Gregory et al., 2015), indicating how the climate in FLOR is more unstable at the end of the cooling experiments due to destabilizing atmospheric feedbacks despite higher OHUE (Figure 2e), compared to CM2.1 which is more stable (Figure 2f).

3.2. Sea Ice Response and Ocean Heat Uptake

The ice-albedo feedback contributes most to the feedback differences between FLOR and CM2.1 in the −6% Solar experiments (Figure S2 in Supporting Information S1). In FLOR, this feedback grows rapidly due to faster sea ice expansion (Figure 3a, Figure S3 in Supporting Information S1), with ice nearly reaching the equator in the south Atlantic before the model crashes. Sea surface temperatures also cool more and faster in FLOR than CM2.1, including in the tropics (Figure S4 in Supporting Information S1). The differences are not only due to FLOR's faster ice growth, but also sea ice loss in CM2.1. While ice expands at high latitudes in the Southern Hemisphere and north Atlantic (Figure 3b, Figure S3 in Supporting Information S1), it retreats in the north Pacific for a few

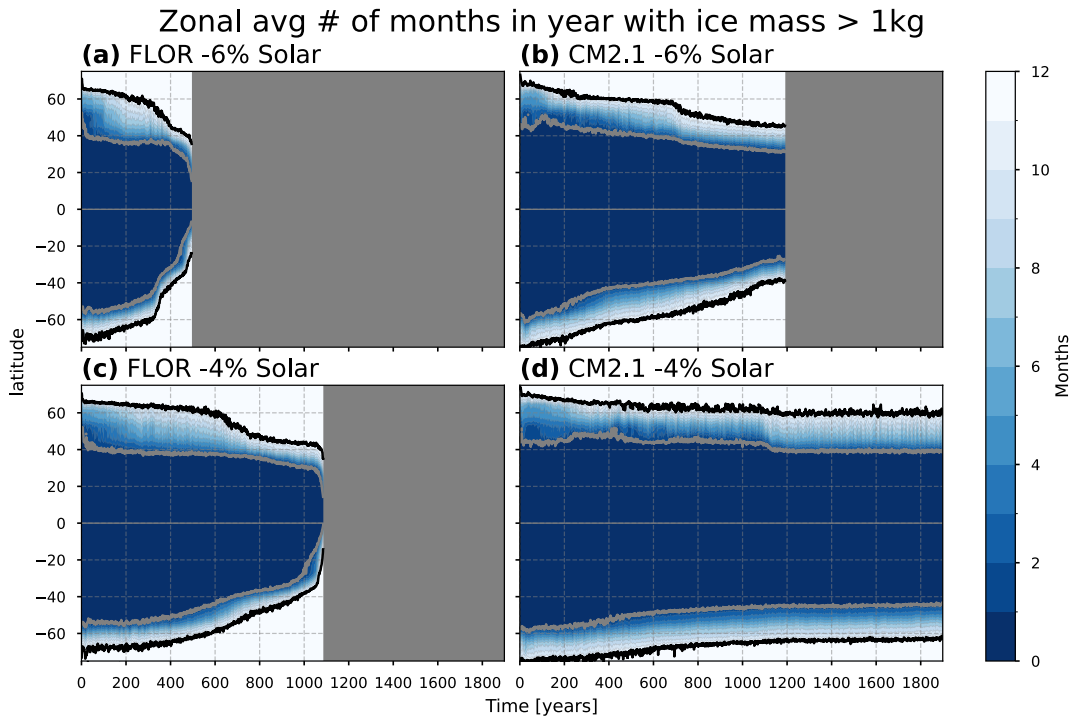

Figure 3. Hovmöller diagrams of the zonal mean number of months per year with sea ice mass >1 kg for the −6% Solar experiments in (a) CM2.5 Forecast-oriented Low Ocean Resolution (FLOR) model and (b) CM2.1, and the −4% Solar experiments in (c) FLOR and (d) CM2.1. Gray lines mark seasonal ice edge and black lines mark perennial ice edge. Gray shading indicates model crashes.

centuries in the −4% and −6% Solar experiments (Figures S5b, S5d in Supporting Information S1), despite globally cold conditions.

To further explore the stabilizing role of OHU in CM2.1, we compare heat content changes in the upper and deep ocean layers. Global total ocean heat content over time can be written as the sum of contributions from the upper and deep ocean:

$$\mathrm{OHC}(t) = \rho c_p (hT(t) + HT_d(t)) \tag{5}$$

where ρ is a reference density, c_p is the specific heat capacity of seawater, h and H are the thicknesses of the upper and deep ocean layers, and $T(t)$ and $T_d(t)$ are their respective temperatures.

Ocean heat uptake (OHU) is given by the time derivative of OHC:

$$\mathrm{OHU}(t) = \rho c_p \left(h \frac{\mathrm{d}T(t)}{\mathrm{d}t} + H \frac{\mathrm{d}T_d(t)}{\mathrm{d}t} \right) \tag{6}$$

We compute the ratio of deep to upper OHU to assess the contribution of each, averaged over time (denoted by $\langle\rangle$):

$$\frac{\mathrm{OHU}_d}{\mathrm{OHU}} = \frac{H}{h} \cdot \frac{\left\langle \frac{\mathrm{d}T_d(t)}{\mathrm{d}t} \right\rangle}{\left\langle \frac{\mathrm{d}T(t)}{\mathrm{d}t} \right\rangle} \tag{7}$$

This ratio is plotted in Figure 4, showing that for the extreme warming and cooling experiments, CM2.1 is more efficient than FLOR at transporting both heat and cold into the deep ocean (>1,000 m) relative to the surface ocean (<1,000 m). These inter-model differences are qualitatively consistent for other depth thresholds between

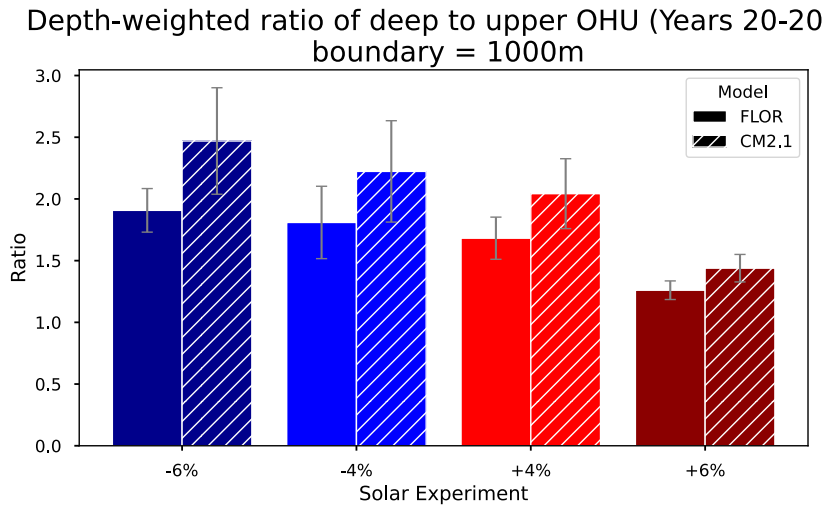

Figure 4. Depth-weighted ratio of deep ocean (below 1,000 m) to upper ocean (0–1,000 m) ocean heat uptake averaged over experiment years 20–200. Solid bars: CM2.5 Forecast-oriented Low Ocean Resolution (FLOR) model. Hatched bars: CM2.1. Gray error bars indicate standard error across years.

the upper and deep ocean, such as 500 m or 200 m. The relatively large deep OHU likely helps to stabilize surface temperatures in CM2.1. The ratio is higher for the cooling experiments than the warming experiments, which is expected because surface cooling leads to higher density waters penetrating deeper into the ocean, whereas surface warming increases stratification and is less likely to affect the deep ocean.

Zonally integrated temperature anomalies in the −6% Solar experiments show spatial heterogeneity in OHU (Figure S6 in Supporting Information S1). The differences between FLOR and CM2.1 tend to be largest in the non-Atlantic basins. CM2.1 cools more below 1,000 m, especially in the tropics and subtropics outside the Atlantic, while FLOR cools more above 1,000 m. However, in the North Pacific (25–60°N), CM2.1 cools much less than FLOR at all depths, suggesting the impact of major differences in Pacific Ocean circulation.

3.3. Pacific Meridional Overturning Circulation

In CM2.1, a PMOC develops within decades in the −4% and −6% Solar experiments, strengthening to about 25 and 45 Sv over a few centuries in each experiment, respectively (Figure S7 in Supporting Information S1). The PMOC drives northward meridional heat transport (calculated as in Msadek et al. (2013)) of approximately 0.6 and 0.8 PW across 40°N in the Pacific (Figure 5a, Figure S8 in Supporting Information S1). For the same experiments in FLOR, a weaker PMOC eventually forms (15 and 30 Sv), but only after runaway cooling has diminished the vertical temperature gradient, thereby limiting the heat transport to about 0.2 PW in both experiments. Both models exhibit long-term AMOC weakening, and in CM2.1 the Pacific becomes the main source of ocean poleward heat transport in the Northern Hemisphere (Figures S7, S8 in Supporting Information S1).

We hypothesize that the PMOC in CM2.1 is enabled by enhanced winter vertical diffusivity in the North Pacific (Figures 5b and 5d). The vertical diffusivity of temperature presented here is an output from the GCMs. It arises from the parameterized vertical mixing due to unresolved turbulence, including gravitational instability (i.e., convection), vertical shear-induced mixing (based on a Richardson number criteria), bottom boundary layer mixing, plus a prescribed constant background diffusivity (Griffies et al., 2005; Vecchi et al., 2014).

CM2.1's higher vertical diffusivity may originate from weaker upper ocean stratification in the Control mean state and differences in the stratification's response to cooling (Figure S9 in Supporting Information S1). These stratification differences are likely caused by the models' distinct vertical mixing schemes, which influence how subgrid-scale processes are represented and can shape both the mean state and the response. Importantly, drivers of the stratification differences evolve over time and are related to temperature, salinity, and sea ice changes in complex ways.

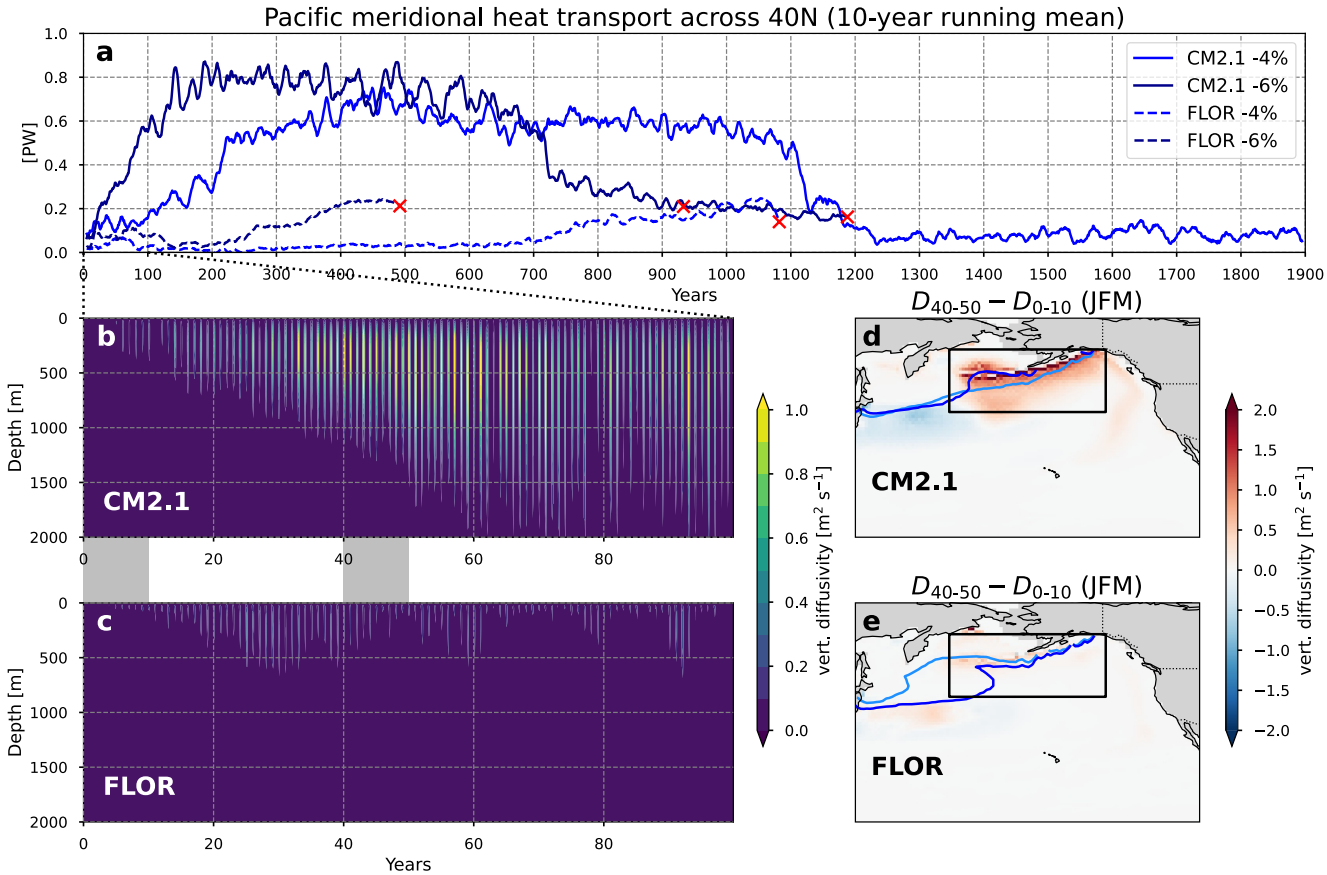

Figure 5. (a) Pacific meridional heat transport across 40°N for −4% (blue) and −6% (dark blue) Solar experiments in CM2.1 (solid) and the CM2.5 Forecast-oriented Low Ocean Resolution (FLOR) model (dashed). Red × marks model crash. (b–e) Vertical diffusivity in the −6% Solar experiments in CM2.1 (b, d) and FLOR (c, e). Hovmöller diagrams of vertical diffusivity with depth, spatially averaged over the boxed region in the maps (d, e) (40°–60°N, 170°E–140°W). Dashed lines indicate that the Hovmöller diagrams show the first 100 years of the experiment. Gray shading between plots (b) and (c) indicate time periods for which vertical diffusivity is compared in the maps (d, e) (years 40–50 minus years 0–10), averaged over January–February–March. Blue contours indicate average sea ice edge positions during years 0–10 (light blue) and 40–50 (dark blue), defined as grid points with ice mass >1 kg in at least one month of the calendar year.

In the Control, the north Pacific in CM2.1 is less stratified than FLOR in the upper 500 m due to temperature (Figures S9a, S9b in Supporting Information S1), because it has a larger temperature inversion (Figure S10 in Supporting Information S1). This appears to precondition CM2.1 for deeper vertical mixing in the upper ocean, which does occur following the −6% Solar change (Figures S9c, S9d in Supporting Information S1). Rapid early sea ice growth in the north Pacific in CM2.1 (Figure S5b in Supporting Information S1) contributes to surface salinification (Figure S11d in Supporting Information S1) and further destabilization via brine rejection. Simultaneously, salinity stratification becomes less stable in CM2.1, likely because subsurface salinity is high in the mean state (more in CM2.1 than FLOR) and mixes up to the surface. Also, the subsurface salinity stratification is weaker in CM2.1, making it easier to erode.

By years 20–30, evidence of the PMOC formation emerges in the north Pacific, including northward meridional heat transport (Figure S11a in Supporting Information S1), sea surface warming (Figures S10, S11c in Supporting Information S1), and sea ice retreat (Figure S5b in Supporting Information S1). Though the surface warming acts to stratify in CM2.1, salinity stratification has already been eroded substantially via mixing with the less-stratified deeper ocean, resulting in salinity-driven destratification. This establishes a positive feedback loop between destratification, vertical mixing, and PMOC strength, which drives further destratification (Figures S9e, S9f in Supporting Information S1).

In contrast, FLOR maintains its halocline near 150 m depth and stronger salinity stratification below 500 m (Figures S9d, S9f in Supporting Information S1), despite cooling more at the surface and producing temperature

inversions (Figure S10 in Supporting Information S1). The strong impact of salinity makes vertical mixing more difficult and delays PMOC formation.

In summary, small initial inter-model differences in upper-ocean stratification in the north Pacific evolved into large differences in PMOC development via interactions with sea ice and ocean mixing. Atmospheric factors such as wind, evaporation, precipitation, and $E - P$ are comparable between the models (Figure S11 in Supporting Information S1). Additionally, historical simulations in both models have weaker stratification than the observed north Pacific (Figure S12 in Supporting Information S1; Locarnini et al. (2017); Zweng et al. (2018)) suggesting that the real ocean circulation may respond differently to extreme cooling.

4. Discussion and Conclusions

This study demonstrates the importance of the sea ice-albedo feedback for climate stability under cooling, consistent with findings from recent work (e.g., Eisenman & Armour, 2024; Kay et al., 2024) and earlier studies using more simplified models. However, unlike those recent GCM studies, we find that nonlinearity in the lapse-rate feedback plays a limited role in our GCM cooling experiments. Instead, in these models, ocean processes such as heat uptake, overturning circulation, and meridional heat transport can significantly impact the sea ice response, especially under strong cooling. These dynamics have received relatively less attention in prior cooling studies. Our results thus highlight that sea ice feedbacks and their implications for climate cannot be fully understood without considering their coupled interactions with the ocean.

The divergence between CM2.1 and FLOR in the Pacific overturning shows how individual model characteristics can shape long-term climate responses. While much attention has been given to AMOC responses under warming (e.g., Baker et al., 2023, 2025; Madan et al., 2024; Weijer et al., 2020), GCM cooling experiments remain relatively rare, resulting in significant uncertainty about the ocean's response to a cooling climate. However, GCM studies on PMOC formation emphasize the role of surface salinification and low subsurface salinity stratification in the north Pacific, which aligns with our results (e.g., Curtis & Fedorov, 2024b; Saenko et al., 2004; Su et al., 2018).

Our findings also demonstrate how the ocean can act as a transient stabilizing feedback, dampening surface temperature changes through ocean circulation and heat uptake. However, these processes can be sensitive to a wide range of factors. The presence or absence of a PMOC in the cooling experiments appeared to be influenced by mean-state stratification differences and the responses of sea ice, temperature, and salinity, which may have stemmed from relatively small differences in model configurations. CM2.1's lower mean-state stratification in the north Pacific may have contributed to its higher OHU efficiency in most of the Solar experiments, as has been suggested in previous work on warming (Newsom et al., 2023), though the PMOC also likely contributes significantly in the extreme cooling scenarios.

Although these two models differ, they are more similar to each other than the full range of coupled models. These sensitivities raise concerns about our ability to predict long-term climate responses across models. The result that seemingly modest differences in parameterizations or mean states can lead to starkly different climate responses demonstrates the need for targeted inter-model comparison. This study showed that two GCMs from the same modeling center exposed to the same external forcing produce dramatically different transient and equilibrium responses. These discrepancies may be indicative of understudied uncertainties about fundamental feedbacks within the climate system. By systematically comparing how climate models simulate ice–ocean interactions and their coupling to atmospheric feedbacks, we may further characterize key sensitivities, reduce uncertainty, and better constrain future projections.

Though the solar forcing experiments in this study are idealized, they provide important insights into the dynamics of long-term climate responses. Abrupt changes of these magnitudes are unrealistic and therefore have limited direct applicability to more realistic climate cooling scenarios (e.g., paleoclimate, large volcanic eruptions, geoengineering), but our results motivate exploration of ocean circulation changes and impacts on climate in those types of studies. This work reveals feedbacks that evolve on multi-century timescales, particularly in the ocean, and demonstrate need for systematically longer climate model simulations (Rugenstein & Armour, 2021; Rugenstein et al., 2019).

They also test the physical realism and consistency of climate models under large perturbations. Whether FLOR or CM2.1 better represents the real Earth system is unclear. FLOR is a later-generation model and has higher

atmospheric resolution, but both models are tuned to represent near-present climate, and may not be equipped to accurately simulate extreme climate changes. In addition, mean-state differences between models or compared to observations can lead to fundamentally different climate responses, as shown in this study.

This work demonstrates the value of cooling-focused experiments as a complement to the more common warming scenarios, and the need for model inter-comparison to better understand climate feedbacks under cooling. Studying climate cooling offers insights into past climates and potential future climate scenarios, as well as asymmetric processes and thresholds that might be missed in warming contexts. Coordinated efforts to explore these questions across a range of forcing scenarios and climate models is therefore essential to assess model performance and understand the fundamental behavior of our climate.

Conflict of Interest

The authors declare no conflicts of interest relevant to this study.

Data Availability Statement

Data for generating figures in this work are available on Zenodo under a Creative Commons Attribution 4.0 International license (Chung, 2025a). Code for running the analysis and creating the figures is published on Github and licensed under MIT (Chung, 2025b).

Acknowledgments
This work is supported by the National Science Foundation Graduate Research Fellowship Program under Grant DGE-2039656; the Carbon Mitigation Initiative at Princeton University funded by BP International; National Aeronautics and Space Administration award 80NSSC20K0879; and the Simons Foundation. Any opinions, findings, and conclusions or recommendations expressed in this material are those of the authors and do not necessarily reflect the views of the National Science Foundation. The simulations presented in this paper were performed on computational resources managed and supported by Princeton Research Computing at Princeton University.

References

Armour, K. C., Bitz, C. M., & Roe, G. H. (2013). Time-varying climate sensitivity from regional feedbacks. *Journal of Climate*, *26*(13), 4518–4534. https://doi.org/10.1175/JCLI-D-12-00544.1

Baker, J. A., Bell, M. J., Jackson, L. C., Renshaw, R., Vallis, G. K., Watson, A. J., & Wood, R. A. (2023). Overturning pathways control AMOC weakening in CMIP6 models. *Geophysical Research Letters*, *50*(14), e2023GL103381. https://doi.org/10.1029/2023GL103381

Baker, J. A., Bell, M. J., Jackson, L. C., Vallis, G. K., Watson, A. J., & Wood, R. A. (2025). Continued Atlantic overturning circulation even under climate extremes. *Nature*, *638*(8052), 987–994. https://doi.org/10.1038/s41586-024-08544-0

Bonan, D. B., Thompson, A. F., Newsom, E. R., Sun, S., & Rugenstein, M. (2022). Transient and equilibrium responses of the Atlantic overturning circulation to warming in coupled climate models: The role of temperature and salinity. https://doi.org/10.1175/JCLI-D-21-0912.1

Budyko, M. I. (1969). The effect of solar radiation variations on the climate of the Earth. *Tellus*, *21*(5), 611–619. https://doi.org/10.3402/tellusa.v21i5.10109

Chung, M. V. (2025a). Runaway cooling from large solar reductions modulated by ocean overturning circulation and heat uptake [Dataset]. *Zenodo*. https://doi.org/10.5281/zenodo.15786791

Chung, M. V. (2025b). mayavchung/solar-change [Software]. *Zenodo*. https://doi.org/10.5281/zenodo.15758199

Curtis, P. E., & Fedorov, A. V. (2024a). Collapse and slow recovery of the atlantic meridional overturning circulation (AMOC) under abrupt greenhouse gas forcing. *Climate Dynamics*, *62*(7), 5949–5970. https://doi.org/10.1007/s00382-024-07185-3

Curtis, P. E., & Fedorov, A. V. (2024b). Spontaneous activation of the Pacific meridional overturning circulation (PMOC) in long-term ocean response to greenhouse forcing. *Journal of Climate*, *37*(5), 1551–1565. https://doi.org/10.1175/JCLI-D-23-0393.1

Delworth, T. L., Broccoli, A. J., Rosati, A., Stouffer, R. J., Balaji, V., Beesley, J. A., et al. (2006). GFDL's CM2 global coupled climate models. Part I: Formulation and simulation characteristics. *Journal of Climate*, *19*(5), 643–674. https://doi.org/10.1175/JCLI3629.1

Eisenman, I., & Armour, K. C. (2024). The radiative feedback continuum from snowball Earth to an ice-free hothouse. *Nature Communications*, *15*(1), 6582. https://doi.org/10.1038/s41467-024-50406-w

Gregory, J. M., Andrews, T., & Good, P. (2015). The inconstancy of the transient climate response parameter under increasing CO2. *Philosophical Transactions of the Royal Society A: Mathematical, Physical and Engineering Sciences*, *373*(2054), 20140417. https://doi.org/10.1098/rsta.2014.0417

Griffies, S. M., Gnanadesikan, A., Dixon, K. W., Dunne, J. P., Gerdes, R., Harrison, M. J., et al. (2005). Formulation of an ocean model for global climate simulations. *Ocean Science*, *1*(1), 45–79. https://doi.org/10.5194/os-1-45-2005

Haskins, R. K., Oliver, K. I. C., Jackson, L. C., Drijfhout, S. S., & Wood, R. A. (2019). Explaining asymmetry between weakening and recovery of the AMOC in a coupled climate model. *Climate Dynamics*, *53*(1), 67–79. https://doi.org/10.1007/s00382-018-4570-z

Held, I. M., Linder, D. I., & Suarez, M. J. (1981). Albedo feedback, the meridional structure of the effective heat diffusivity, and climatic sensitivity: Results from dynamic and diffusive models. *Journal of the Atmospheric Sciences*, *38*(9), 1911–1927. https://doi.org/10.1175/1520-0469(1981)038⟨1911:AFTMSO⟩2.0.CO;2

Held, I. M., & Shell, K. M. (2012). Using relative humidity as a state variable in climate feedback analysis. *Journal of Climate*, *25*(8), 2578–2582. https://doi.org/10.1175/JCLI-D-11-00721.1

Held, I. M., & Suarez, M. J. (1974). Simple albedo feedback models of the icecaps. *Tellus*, *26*(6), 613–629. https://doi.org/10.1111/j.2153-3490.1974.tb01641.x

Held, I. M., Winton, M., Takahashi, K., Delworth, T., Zeng, F., & Vallis, G. K. (2010). Probing the fast and slow components of global warming by returning abruptly to preindustrial forcing. *Journal of Climate*, *23*(9), 2418–2427. https://doi.org/10.1175/2009JCLI3466.1

Jansen, M. F., Nadeau, L.-P., & Merlis, T. M. (2018). Transient versus equilibrium response of the ocean's overturning circulation to warming. https://doi.org/10.1175/JCLI-D-17-0797.1

Kay, J. E., Liang, Y.-C., Zhou, S.-N., & Maher, N. (2024). Sea ice feedbacks cause more greenhouse cooling than greenhouse warming at high northern latitudes on multi-century timescales. *Environmental Research: Climate*, *3*(4), 041003. https://doi.org/10.1088/2752-5295/ad8026

Locarnini, M., Mishonov, A., Baranova, O., Boyer, T., Zweng, M., Garcia, H., et al. (2017). World ocean atlas 2018, volume 1: Temperature. *World Ocean Atlas*. Retrieved from https://archimer.ifremer.fr/doc/00651/76338/

Madan, G., Gjermundsen, A., Iversen, S. C., & LaCasce, J. H. (2024). The weakening AMOC under extreme climate change. *Climate Dynamics*, *62*(2), 1291–1309. https://doi.org/10.1007/s00382-023-06957-7

Mitevski, I., Orbe, C., Chemke, R., Nazarenko, L., & Polvani, L. M. (2021). Non-monotonic response of the climate system to abrupt CO2 forcing. *Geophysical Research Letters*, *48*(6), e2020GL090861. https://doi.org/10.1029/2020GL090861

Msadek, R., Johns, W. E., Yeager, S. G., Danabasoglu, G., Delworth, T. L., & Rosati, A. (2013). The Atlantic meridional heat transport at 26.5°N and its relationship with the MOC in the RAPID array and the GFDL and NCAR coupled models. https://doi.org/10.1175/JCLI-D-12-00081.1

Newsom, E., Zanna, L., & Gregory, J. (2023). Background pycnocline depth constrains future ocean heat uptake efficiency. *Geophysical Research Letters*, *50*(22), e2023GL105673. https://doi.org/10.1029/2023GL105673

Proistosescu, C., & Huybers, P. J. (2017). Slow climate mode reconciles historical and model-based estimates of climate sensitivity. *Science Advances*, *3*(7), e1602821. https://doi.org/10.1126/sciadv.1602821

Rose, B. E. J., Armour, K. C., Battisti, D. S., Feldl, N., & Koll, D. D. B. (2014). The dependence of transient climate sensitivity and radiative feedbacks on the spatial pattern of ocean heat uptake. *Geophysical Research Letters*, *41*(3), 1071–1078. https://doi.org/10.1002/2013GL058955

Rugenstein, M., & Armour, K. C. (2021). Three flavors of radiative feedbacks and their implications for estimating equilibrium climate sensitivity. *Geophysical Research Letters*, *48*(15), e2021GL092983. https://doi.org/10.1029/2021GL092983

Rugenstein, M., Bloch-Johnson, J., Abe-Ouchi, A., Andrews, T., Beyerle, U., Cao, L., et al. (2019). LongRunMIP: Motivation and design for a large collection of millennial-length AOGCM simulations. *Bulletin of the American Meteorological Society*, *100*(12), 2551–2570. https://doi.org/10.1175/BAMS-D-19-0068.1

Saenko, O. A., Schmittner, A., & Weaver, A. J. (2004). The Atlantic–Pacific seesaw. *Journal of Climate*, *17*(11), 2033–2038. https://doi.org/10.1175/1520-0442(2004)017<2033:tas>2.0.co;2

Sellers, W. D. (1969). A global climatic model based on the energy balance of the earth-atmosphere system. *Journal of Applied Meteorology and Climatology*, *8*(3), 392–400. https://doi.org/10.1175/1520-0450(1969)008⟨0392:AGCMBO⟩2.0.CO;2

Sellers, W. D. (1983). A quasi-three-dimensional climate model. *Journal of Applied Meteorology and Climatology*, *22*(9), 1557–1574. https://doi.org/10.1175/1520-0450(1983)022<1557:aqtdcm>2.0.co;2

Sellers, W. D. (1985). The effect of a solar perturbation on a global climate model. *Journal of Applied Meteorology and Climatology*, *24*(8), 770–776. https://doi.org/10.1175/1520-0450(1985)024<0770:teoasp>2.0.co;2

Soden, B. J., Held, I. M., Colman, R., Shell, K. M., Kiehl, J. T., & Shields, C. A. (2008). Quantifying climate feedbacks using radiative kernels. *Journal of Climate*, *21*(14), 3504–3520. https://doi.org/10.1175/2007JCLI2110.1

Stouffer, R. J. (2004). Time scales of climate response. *Journal of Climate*, *17*(1), 209–217. https://doi.org/10.1175/1520-0442(2004)017⟨0209:TSOCR⟩2.0.CO;2

Stouffer, R. J., & Manabe, S. (2003). Equilibrium response of thermohaline circulation to large changes in atmospheric CO2 concentration. *Climate Dynamics*, *20*(7), 759–773. https://doi.org/10.1007/s00382-002-0302-4

Su, B., Jiang, D., Zhang, R., Sepulchre, P., & Ramstein, G. (2018). Difference between the north Atlantic and Pacific meridional overturning circulation in response to the uplift of the Tibetan Plateau. *Climate of the Past*, *14*(6), 751–762. https://doi.org/10.5194/cp-14-751-2018

Vecchi, G. A., Delworth, T., Gudgel, R., Kapnick, S., Rosati, A., Wittenberg, A. T., et al. (2014). On the seasonal forecasting of regional tropical cyclone activity. *Journal of Climate*, *27*(21), 7994–8016. https://doi.org/10.1175/JCLI-D-14-00158.1

Wang, C., Yang, W., Vecchi, G., Zhang, B., Soden, B. J., & Chan, D. (2025). Diagnosing the factors that contribute to the intermodel spread of climate feedback in CMIP6. *Journal of Climate*, *38*(3), 663–674. https://doi.org/10.1175/JCLI-D-23-0528.1

Weijer, W., Cheng, W., Garuba, O. A., Hu, A., & Nadiga, B. T. (2020). CMIP6 models predict significant 21st century decline of the Atlantic meridional overturning circulation. *Geophysical Research Letters*, *47*(12), e2019GL086075. https://doi.org/10.1029/2019GL086075

Wetherald, R. T., & Manabe, S. (1975). The effects of changing the solar constant on the climate of a general circulation model. *Journal of the Atmospheric Sciences*, *32*(11), 2044–2059. https://doi.org/10.1175/1520-0469(1975)032⟨2044:TEOCTS⟩2.0.CO;2

Winton, M., Takahashi, K., & Held, I. M. (2010). Importance of ocean heat uptake efficacy to transient climate change. *Journal of Climate*, *23*(9), 2333–2344. https://doi.org/10.1175/2009JCLI3139.1

Zweng, M., Reagan, J., Seidov, D., Boyer, T., Locarnini, M., Garcia, H., et al. (2018). World ocean atlas 2018, volume 2: Salinity. *World Ocean Atlas*. Retrieved from https://archimer.ifremer.fr/doc/00651/76339/